

Use of finite and infinite elements in static analysis of pavement

V.A. Patil^{1*}, V.A. Sawant¹ and Kousik Deb²

¹*Department of Civil Engineering, Indian Institute of Technology Roorkee,
Roorkee-247667, Uttarakhand, India*

²*Department of Civil Engineering, Indian Institute of Technology Kharagpur, Kharagpur-721302, India*

(Received November 5, 2009, Accepted January 20, 2010)

Abstract. In recent years, study of the static response of pavements to moving vehicle and aircraft loads has received significant attention because of its relevance to the design of pavements and airport runways. The static response of beams resting on an elastic foundation and subjected to moving loads was studied by several researchers in the past. However, most of these studies were limited to steady-state analytical solutions for infinitely long beams resting on Winkler-type elastic foundations. Although the modelling of subgrade as a continuum is more accurate, such an approach can hardly be incorporated in analysis due to its complexity. In contrast, the two-parameter foundation model provides a better way for simulating the underlying soil medium and is conceptually more appealing than the one-parameter (Winkler) foundation model. The finite element method is one of the most suitable mathematical tools for analysing rigid pavements under moving loads. This paper presents an improved solution algorithm based on the finite element method for the static analysis of rigid pavements under moving vehicular or aircraft loads. The concrete pavement is discretized by finite and infinite beam elements, with the latter for modelling the infinity boundary conditions. The underlying soil medium is modelled by the Pasternak model allowing the shear interaction to exist between the spring elements. This can be accomplished by connecting the spring elements to a layer of incompressible vertical elements that can deform in transverse shear only. The deformations and forces maintaining equilibrium in the shear layer are considered by assuming the shear layer to be isotropic. A parametric study is conducted to investigate the effect of the position of moving loads on the response of pavement.

Keywords: beam element; damping; foundation; moving loads; pavement; Pasternak's model; subgrade.

1. Introduction

Generally, in the analysis of bending of beams on an elastic foundation, the subgrade models such as the Winkler, Filenenko-Borodich, Pasternak, Vlasov, Reissner, Hetenyi, etc., play a very important role. The salient features of the original problem are retained in the model and the gross behaviour of the beam-foundation system can be investigated to highlight the major parameters and characteristics of the problem

* Corresponding author, Research Scholar, E-mail: vikrampatil70@gmail.com

The analysis of bending of beams on an elastic foundation is developed on the assumption that the reaction forces of the foundation are proportional at every point to the deflection of the beam at that point. This assumption was first introduced by Winkler (1867), which formed the basis of Zimmermann's (1930) classical work on the analysis of railroad tracks. The Winkler model has been extensively applied for the analysis of both shallow and deep foundations. It has been shown by Foppl's (1922) classical experiment and Hetenyi's (1950) analytical work that Winkler's assumption, in spite of its simplicity, leads to satisfactory results in the stress analysis of beams resting on an elastic foundation. On the other hand, by means of the hypothesis of isotropic, linearly elastic semi-infinite space, the physical properties of a natural foundation can be correctly described. To bridge the gap between these two extreme cases, interactions between Winkler's springs were considered by several authors. Hetenyi (1950, 1946) treated the problems of beams or plates on an elastic foundation by assuming a continuous beam or plate imbedded in the material of foundation, which is itself without any continuity. Pasternak (1954) assumed that the shear interactions exist between the springs. Vlasov and Leont'ev (1966) also considered the shear interactions in the foundation and formulated their problems by using a variational method. A number of studies report the applicability of two-parameter models (Pasternak and Vlasov). They solved a large number of problems involving beams, plates and shells on elastic foundation. The foundation considered is the two-parameter model with the shear interactions taken into account.

Sun (2001) presented a closed form solution for the response of a beam resting on a Winkler foundation subjected to a moving line load, by means of two-dimensional Fourier transform and using Green's function. Shen and Kirkner (2001) presented a nonlinear 3D finite element analysis to treat the involved nonlinear boundary conditions and to allow accurate prediction of residual displacements. Analysis of a beam resting on reinforced granular bed overlying a soft soil strata subjected to a moving load with constant velocity was presented by Maheswari *et al.* (2004). The steady-state response of a uniform beam placed on an elastic foundation and subjected to a concentrated load moving with a constant speed has been investigated by Mallik *et al.* (2006). An effort has been made to find the solution of the governing differential equation analytically with and without viscous damping. A meshless formulation using element free Galerkin method is presented by Sunitha *et al.* (2008) to solve the governing differential equation of the beams on elastic foundation.

In the recent years more attention is given to the establishment of more realistic foundation models and development of simplified methods for analyzing complex structures, taking into account the elasticity of foundations.

An approximate numerical approach, based on the finite element technique, is appropriate for analyzing complex structures resting on an elastic foundation, since it leads to relatively straightforward matrix expressions. For the computation of long and complicated numerical results, one can rely upon the modern digital computer. Besides, due to the versatility of the finite element method, the variations in the geometry, loading and boundary conditions of the structure can be easily taken into account. This paper presents a solution algorithm based on finite element method for analyzing rigid pavements under moving vehicular or aircraft loads. The concrete pavement is discretized by the beam elements. The underlying soil medium is modeled by the Pasternak model allowing the shear interaction to exist between the spring elements. This can be accomplished by connecting the spring elements to a layer of incompressible vertical elements that can deform in transverse shear only. The deformations and forces maintaining equilibrium in the shear layer are considered by assuming the shear layer as an isotropic material. In addition to the conventional

element stiffness matrix, two additional matrices are derived for a beam element lying on an elastic foundation: (i) the 'compressive stiffness' matrix of the foundation, which is similar to the conventional 'consistent mass' matrix, to account for the spring effects of the foundation, and (ii) the 'friction stiffness' matrix of the foundation, which is somewhat similar to the conventional 'initial stress' matrix, to account for the shear interactions of the foundation beneath the beam. The development of the infinite elements has helped in modeling the far field behavior and also in reducing the number of elements and hence computational cost (Bettess 1977). A parametric study is conducted to investigate the effect of moving loads on the response of pavement.

2. Beam on an elastic foundation with Pasternak model

A single-layer elastic foundation of finite thickness H is considered (see Fig. 1). The subject matter will be restricted to the problems where the horizontal displacement is negligible. In addition, it is assumed that the shear stress at the interface between the compressible layer and the rigid base equals zero. For a relatively thin compressible layer of foundation, the variation of the normal stresses along the depth may be small and therefore can be considered as constant with depth. Based on the conventional stress-strain and strain-displacement relationships, the equilibrium of an infinitesimal element of the foundation under an externally distributed load $q(x)$ as shown in Fig. 1 can be given by the following differential equation

$$q(x) = -G_p b H \frac{d^2 w}{dx^2} + k b w \quad (1)$$

Consider a beam resting on an elastic single-layer foundation whose properties are as described previously. By neglecting the friction and adhesion between the beam and foundation surface, the differential equation for bending of the beam is

$$EI \frac{d^4 w}{dx^4} = \bar{p}(x) \quad (2)$$

in which $\bar{p}(x)$ is the distributed load on the beam and EI is the flexural rigidity of the beam. Since the beam lies on an elastic foundation, the distributed load consists of the given surface loads $p(x)$ and the foundation bearing pressure $q(x)$

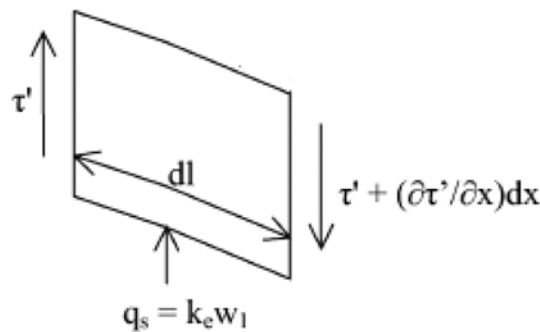


Fig. 1 Pasternak's two parameter model

$$\bar{p}(x) = p(x) - q(x) \quad (3)$$

Substitution of Eqs. (1) and (3) into Eq. (2) yields

$$EI \frac{d^4 w}{dx^4} - G_p b H \frac{d^2 w}{dx^2} + k b w = p(x) \quad (4)$$

An examination of above equation shows that the first term depends on the internal bending stresses in the beam, while the second and third terms depend on the reactions of the elastic foundation, distributed over the surface supporting the beam and caused by the compressive and shearing strains in the elastic foundation.

3. Finite element stiffness formulation

The equilibrium equation of a beam lying on an elastic foundation has been shown in the preceding section (Eq. 4). The strain energy U of the system can be expressed as follows

$$U = \frac{1}{2} \int_0^L \left(EI \left(\frac{d^2 w}{dx^2} \right) \times \left(\frac{d^2 w}{dx^2} \right) - G_p b H \left(\frac{dw}{dx} \right) \times \left(\frac{dw}{dx} \right) + k b w \times w \right) dx \quad (5)$$

This equation may also be written in a stiffness matrix form for any appropriately developed beam finite element as follows

$$[[k_1] + [k_2] + [k_3]] \{ \delta \} = \{ f \} \quad (6)$$

in which $\{f\}$ is the vector of nodal loads, $\{\delta\}$ is the vector of flexural nodal displacements of the element, $[k_1]$ is the conventional element stiffness matrix for beam flexure, corresponding to the term

$EI \frac{d^4 w}{dx^4}$ in Eq. (4), $[k_2]$ is the friction stiffness matrix of the foundation underlying the beam element, corresponding to the term $G_p b H \frac{d^2 w}{dx^2}$ in Eq. (4), and $[k_3]$ is compressive stiffness matrix of the foundation,

corresponding to the term $k b w$ in Eq. (4).

It is of interest to point out that Eq. (5) can be visualized as an equilibrium equation of motion of a freely vibrating beam with a harmonic frequency equal to unity and a beam mass density equal to k , while the beam is subjected to a pair of orthogonal in-plane compressive stresses equal to G_p (no in-plane shear). With this analogy in mind, it is clear that the ‘friction stiffness’ matrix $[k_2]$ of the foundation beneath the beam element is similar to the ‘initial stress’ matrix for the buckling and large deflection analysis of a beam, for which the two orthogonal in-plane stresses equal to G_p and the in-plane shearing stress vanishes. It is also clear that the ‘compressive stiffness’ matrix $[k_3]$ of the foundation beneath the beam element is identical to the ‘consistent mass’ matrix of a freely vibrating beam element where the mass density is replaced by the compressive spring constant k and the natural frequency is set to unity.

The matrices $[k_1]$, $[k_2]$ and $[k_3]$ can be computed as follows

$$[k_1] = \int_0^L \left(\left[\frac{d^2 N}{dx^2} \right]^T EI \left[\frac{d^2 N}{dx^2} \right] \right) dx$$

$$[k_2] = \int_0^L \left(\left[\frac{dN}{dx} \right]^T G_p b H \left[\frac{dN}{dx} \right] \right) dx \quad (7)$$

$$[k_3] = \int_0^L ([N]^T k b [N]) dx$$

3.1 Finite Element

In case of finite beam element, the shape functions are

$$[N] = [1 - 3\xi^2 + 2\xi^3 \quad \xi(1 - 2\xi + \xi^2)L \quad 3\xi^2 - 2\xi^3 \quad \xi(-\xi + \xi^2)L] \quad (8)$$

3.2 Infinite Element

The main purpose of the development of infinite elements is to model the unbounded domain. Bettess presented a general approach for deriving the infinite elements from the finite element (parent element). The shape functions of the finite element are multiplied by a decay function. The role of the decay function is to ensure that the behaviour of the element at infinity is reasonable reflection of the physical characteristics of the problem considered. This means that the far field variable should approach monotonically to its far field value. The decay function employed in the present study is an exponential decay function, with which the finite element shape functions are modified as follows

$$[N] = \left[(1 - 3\xi^2 + 2\xi^3)e^{-n\xi} \quad L(\xi - 2\xi^2 + \xi^3)e^{-n\xi} \quad (3\xi^2 - 2\xi^3)e^{n(1-\xi)} \quad L(-\xi^2 + \xi^3)e^{n(1-\xi)} \right] \quad (9)$$

The matrices $[k_1]$, $[k_2]$ and $[k_3]$ can be derived from same Eq. (7) using numerical integration. Before carrying out numerical integration using the two point Gauss quadrature, the integrals involved have to be converted to those with limits varying between -1 to 1 . The following is the conversion adopted in this study

$$[k] = \int_0^\infty (f(x)) dx = \int_0^\infty (f(\xi)) L d\xi = \int_{-1}^1 f \left(\sqrt{\frac{1-t}{1+t}} \right) \frac{L}{(1+t)\sqrt{1-t^2}} dt$$

where $\xi = \frac{x-x_1}{L}$ and $\xi = \sqrt{\frac{1-t}{1+t}}$

$$t_1 = -\frac{1}{\sqrt{3}}; \xi_1 = 1.931852 \quad \text{and} \quad t_2 = -\frac{1}{\sqrt{3}}; \xi_2 = 0.517638$$

Using the conventional procedure of assemblage, the global stiffness matrix can be established for the entire system as follows

$$[[k_1] + [k_2] + [k_3]]\{d\} = \{F\} \quad \text{OR} \quad [K^*]\{d\} = \{F\} \quad (10)$$

4. Validation

To verify the accuracy of the above finite element formulation and the computer program

Table 1 Validation of finite beam

	Central Deflection (mm)		Central Moment (kNm)	
	Winkler	Two-Parameter	Winkler	Two-Parameter
Analytical	1.5585	1.506813	94.71465	89.27447
FEM	1.5585	1.506800	94.714	89.274
Error	0.0	0.0009	0.0	0.0005

Table 2 Validation of infinite beam

	Central Deflection (mm)		Central Moment (kNm)	
	Winkler	Two-Parameter	Winkler	Two-Parameter
Analytical	1.4282	1.3891	87.5213	85.1241
FEM	1.4362	1.3944	87.5213	85.2180
Error	0.5584	0.3811	0.0	0.1103

developed, the response of a beam computed is compared with standard closed form solutions available. The closed form solutions for beams resting on an elastic foundation with Winkler model and two parameter model are available. The following material properties are adopted in the analysis for validation and parametric study.

- Beam $L = 10$ m, $b = 1$ m, $E_b = 0.3605 \times 10^8$ kN/m²
- Soil $G_p = 7000$ kN/m², $k = 10000$ kN/m³, $H = 1$ m
- Load $P = 100$ kN

4.1 Winkler's model

To compare the result for beams resting on elastic foundation with Winkler model, G_p is taken equal to zero. For comparison, the beam response in terms of central deflection, end deflection and central moment are considered. In Tables 1 and 2, the results from the finite element analysis are compared with the closed form solution available in literature. Good agreement is observed between the two results.

4.2 Pasternak's model

The response for the condition of a load P applied at the central position is considered for comparison. The governing differential Eq. (4) is solved analytically as described below.

$$EI \frac{d^4 w}{dx^4} - G_p b H \frac{d^2 w}{dx^2} + k b w = 0$$

The solution of the above equation and its higher derivatives are given as follows

$$\begin{aligned}
w &= e^{-\lambda\mu x}(C_1 \cos(\lambda\beta x) + C_2 \sin(\lambda\beta x)) + e^{\lambda\mu x}(C_3 \cos(\lambda\beta x) + C_4 \sin(\lambda\beta x)) \\
\frac{dw}{dx} &= \lambda \left[e^{-\lambda\mu x} \{(\beta C_2 - \mu C_1) \cos(\lambda\beta x) + (-\beta C_1 - \mu C_2) \sin(\lambda\beta x)\} \right. \\
&\quad \left. + e^{\lambda\mu x} \{(\mu C_3 + \beta C_4) \cos(\lambda\beta x) + (\mu C_4 - \beta C_3) \sin(\lambda\beta x)\} \right] \\
\frac{d^2 w}{dx^2} &= \lambda^2 \left[e^{-\lambda\mu x} \{(\alpha_1 C_1 - \alpha_2 C_2) \cos(\lambda\beta x) + (\alpha_1 C_2 + \alpha_2 C_1) \sin(\lambda\beta x)\} \right. \\
&\quad \left. + e^{\lambda\mu x} \{(\alpha_1 C_3 + \alpha_2 C_4) \cos(\lambda\beta x) + (\alpha_1 C_4 - \alpha_2 C_3) \sin(\lambda\beta x)\} \right] \\
\frac{d^3 w}{dx^3} &= \lambda^3 \left[e^{-\lambda\mu x} \{(-\alpha_4 C_1 - \alpha_3 C_2) \cos(\lambda\beta x) + (\alpha_3 C_1 + \alpha_4 C_2) \sin(\lambda\beta x)\} \right. \\
&\quad \left. + e^{\lambda\mu x} \{(\alpha_4 C_3 - \alpha_3 C_4) \cos(\lambda\beta x) + (\alpha_3 C_3 + \alpha_4 C_4) \sin(\lambda\beta x)\} \right]
\end{aligned} \tag{11}$$

$$\text{where } \lambda = \sqrt[4]{\frac{kb}{4EI}} \quad \mu = \sqrt{1 + \frac{G_p H}{k} \lambda^2} \quad \beta = \sqrt{1 - \frac{G_p H}{k} \lambda^2}$$

$$\alpha_1 = (\mu^2 - \beta^2); \alpha_2 = (2\mu\beta); \alpha_3 = (\beta^3 - 3\beta\mu^2); \alpha_4 = (\mu^3 - 3\mu\beta^2)$$

The constants C_1 to C_4 are evaluated using the following four boundary conditions

$$\text{At centre, } x = 0, \frac{dw}{dx} = 0, \text{ which yields } \beta(C_2 + C_4) = \mu(C_1 - C_3)$$

$$\text{At centre, } x = 0, \text{ shear } N = -EI \frac{d^3 w}{dx^3} + G_p b H \frac{dw}{dx} = -\frac{P}{2}, \text{ yielding}$$

$$\frac{P}{2EI\lambda^3} = \alpha_4(C_3 - C_1) - \alpha_3(C_2 + C_4)$$

The above two equations are further simplified as

$$(C_1 - C_3) = \frac{P}{4EI\lambda^3(\mu^2 + \beta^2)\mu} \tag{12}$$

$$(C_2 + C_4) = \frac{P}{4EI\lambda^3(\mu^2 + \beta^2)\beta} \tag{13}$$

$$\text{At end, } x = \frac{L}{2}, M = -EI \frac{d^2 w}{dx^2} = 0, \text{ which gives}$$

$$\left[\begin{aligned}
&\left(\alpha_1 \cos\left(\frac{\lambda\beta L}{2}\right) + \alpha_2 \sin\left(\frac{\lambda\beta L}{2}\right) \right) e^{-\lambda\mu L/2} C_1 + \left(\alpha_1 \sin\left(\frac{\lambda\beta L}{2}\right) - \alpha_2 \cos\left(\frac{\lambda\beta L}{2}\right) \right) e^{-\lambda\mu L/2} C_2 \\
&+ \left(\alpha_1 \cos\left(\frac{\lambda\beta L}{2}\right) - \alpha_2 \sin\left(\frac{\lambda\beta L}{2}\right) \right) e^{\lambda\mu L/2} C_3 + \left(\alpha_1 \sin\left(\frac{\lambda\beta L}{2}\right) + \alpha_2 \cos\left(\frac{\lambda\beta L}{2}\right) \right) e^{\lambda\mu L/2} C_4
\end{aligned} \right] = 0 \tag{14}$$

$$\text{At end, } x = \frac{L}{2}, N = -EI \frac{d^3 w}{dx^3} + G_p b H \frac{dw}{dx} = 0$$

$$\left[\begin{aligned} & \left\{ (\alpha_4(EI\lambda^3) - \mu(G_p b H \lambda)) \cos\left(\frac{\lambda\beta L}{2}\right) - (\alpha_3(EI\lambda^3) + \beta(G_p b H \lambda)) \sin\left(\frac{\lambda\beta L}{2}\right) \right\} e^{-\lambda\mu L/2} C_1 \\ & + \left\{ (\alpha_3(EI\lambda^3) + \beta(G_p b H \lambda)) \cos\left(\frac{\lambda\beta L}{2}\right) + (\alpha_4(EI\lambda^3) - \mu(G_p b H \lambda)) \sin\left(\frac{\lambda\beta L}{2}\right) \right\} e^{-\lambda\mu L/2} C_2 \\ & + \left\{ (-\alpha_4(EI\lambda^3) + \mu(G_p b H \lambda)) \cos\left(\frac{\lambda\beta L}{2}\right) - (\alpha_3(EI\lambda^3) + \beta(G_p b H \lambda)) \sin\left(\frac{\lambda\beta L}{2}\right) \right\} e^{\lambda\mu L/2} C_3 \\ & + \left\{ (\alpha_3(EI\lambda^3) + \beta(G_p b H \lambda)) \cos\left(\frac{\lambda\beta L}{2}\right) + (-\alpha_4(EI\lambda^3) + \mu(G_p b H \lambda)) \sin\left(\frac{\lambda\beta L}{2}\right) \right\} e^{\lambda\mu L/2} C_4 \end{aligned} \right] = 0 \quad (15)$$

The above Eqs. (12) to (15) are solved simultaneously to get the unknown constants C_1 to C_4 . For the case of infinite beams, the constants C_3 and C_4 are zero

$$w = e^{-\lambda\mu x} (C_1 \cos(\lambda\beta x) + C_2 \sin(\lambda\beta x)) \quad (16)$$

$$\frac{dw}{dx} = \lambda e^{-\lambda\mu x} \{ (\beta C_2 - \mu C_1) \cos(\lambda\beta x) + (-\beta C_1 - \mu C_2) \sin(\lambda\beta x) \}$$

Applying the boundary conditions for the slope and shear at the centre point:

$$\text{At centre, } x = 0, \frac{dw}{dx} = 0 \Rightarrow (\beta C_2 - \mu C_1) = 0 \text{ or } C_2 = \frac{\mu}{\beta} C_1$$

from which

$$\frac{dw}{dx} = -\lambda e^{-\lambda\mu x} \left(\frac{\beta^2 + \mu^2}{\beta} \right) C_1 \sin(\lambda\beta x)$$

$$\frac{d^2 w}{dx^2} = -\lambda^2 \left(\frac{\beta^2 + \mu^2}{\beta} \right) C_1 e^{-\lambda\mu x} \{ -\mu \sin(\lambda\beta x) + \beta \cos(\lambda\beta x) \} \quad (17)$$

$$\frac{d^3 w}{dx^3} = \lambda^3 \left(\frac{\beta^2 + \mu^2}{\beta} \right) C_1 e^{-\lambda\mu x} \{ (\beta^2 - \mu^2) \sin(\lambda\beta x) + 2\mu\beta \cos(\lambda\beta x) \}$$

$$\text{At centre, } x = 0, \text{ shear } N = -EI \frac{d^3 w}{dx^3} + G_p b H \frac{dw}{dx} = -\frac{P}{2}$$

$$N = -EI \frac{d^3 w}{dx^3} + G_p b H \times 0 = -\frac{P}{2} \text{ or } EI \frac{d^3 w}{dx^3} = \frac{P}{2} \Rightarrow C_1 = \frac{P}{4EI\lambda^3 \mu (\beta^2 + \mu^2)}$$

Substituting the value of constant C_1 in the equations for the displacement and moment gives

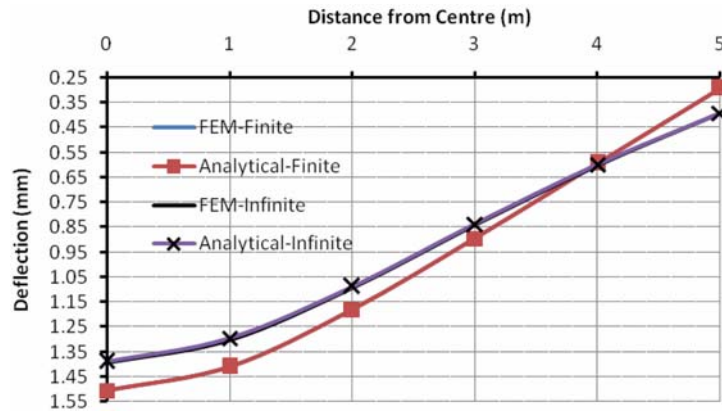


Fig. 2 Comparison of deflected shapes of beam

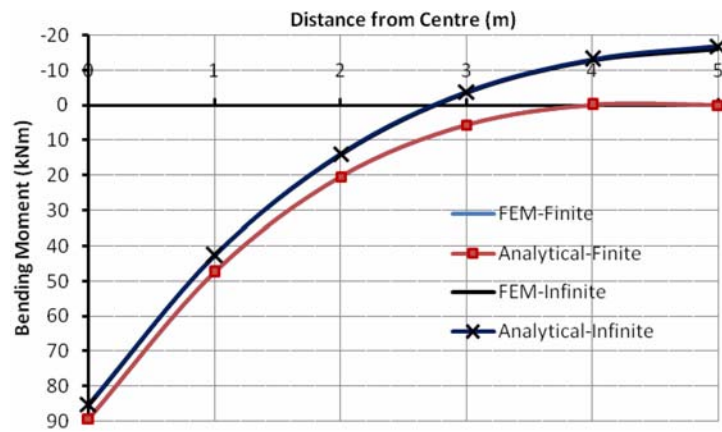


Fig. 3 Comparison of bending moment diagram

$$w = \frac{P}{4EI\lambda^3} \frac{e^{-\lambda\mu x}}{\mu(\beta^2 + \mu^2)} \left(\cos(\lambda\beta x) + \frac{\mu}{\beta} \sin(\lambda\beta x) \right) \quad (18)$$

$$M = \frac{P}{4\beta\lambda\mu} e^{-\lambda\mu x} \{ -\mu \sin(\lambda\beta x) + \beta \cos(\lambda\beta x) \} \quad (19)$$

The deflection and moment at the central point of the beam are used for comparison, as tabulated in Tables 1 and 2. Good agreement is observed between the two solutions. The deflected shape and bending moment diagram for the condition of a load P applied at the central point are presented in Figs. 2 and 3. The deflection curve and bending moment diagram obtained analytically are also shown for comparison.

5. Results

A parametric analysis is conducted to study the effect of selected parameters like the length of beam and shear modulus G_p on the response of beam. The length of the beam is varied from 10 to

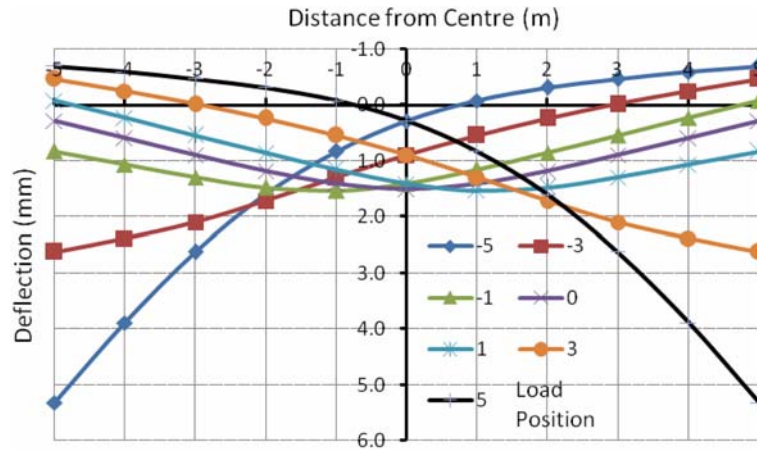


Fig. 4 (a) Deflection response at various load positions for finite 10 m beam

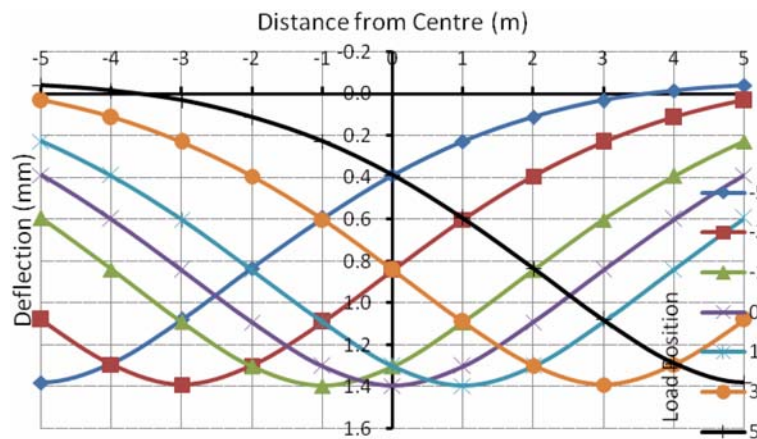


Fig. 4 (b) Deflection response at various load positions for infinite beam

24 m. The analysis is also performed on the infinite beam incorporating the infinite elements on either side. In all the cases, the load position is varied (from -5 to 5 m) in the central span AB of the beam of 10 m length. The properties of two parameter model (k and G_p) adopted are $k = 10000$ (kN/m^3) and $G_p = 7000$ (kN/m^2).

5.1 Effect of load position

The deflection responses to seven different load positions $\{x = -5, -3, -1, 0, 1, 3, 5\}$ are plotted in Figs. 4 (a) and 4 (b) for a 10 m finite beam and infinite beam, respectively. The end deflections are considerably higher for the finite beam. Similar comparison for the moment response is presented in Figs. (5) a and 5 (b). The values of the maximum positive or negative moments vary marginally with the load position for the case of infinite beams, whereas significant variation is observed for the case of finite beams. The effect is more pronounced when the load is placed at end points A or B .

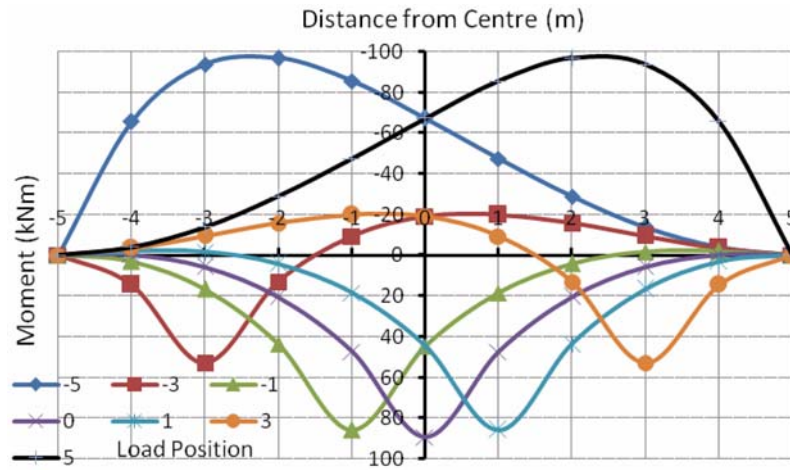


Fig. 5 (a) Moment response at various load positions for finite 10 m beam

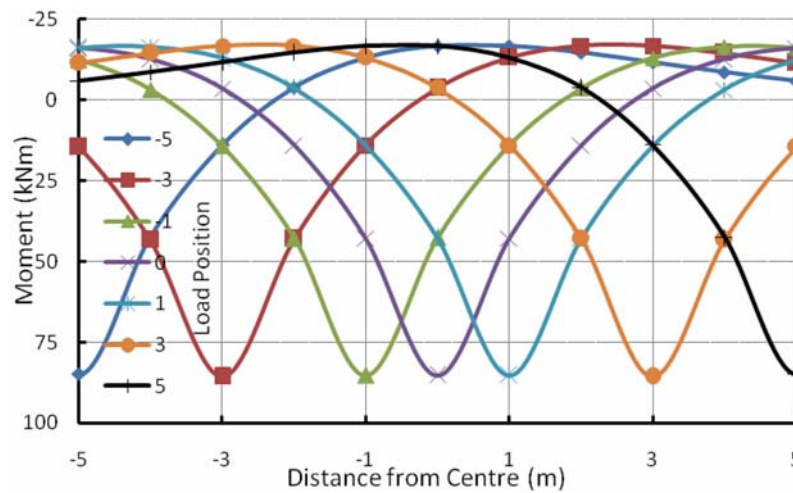


Fig. 5 (b) Moment response at various load positions for infinite beam

The variations in the deflection of point *A*, the central deflection and central moment are considered to highlight the effect of load positions. The effect of load positions on the deflection of the beam at point *A* (starting point of load application) is presented in Fig. 6 for 10 m and 20 m finite beams, and an infinite beam. The deflections are considerably higher for the 10 m beam, but there is not much difference for the case of 20 m beam and infinite beam. Similar comparison for the central deflection is given in Fig. 7. The deflections of the 20 m beam and infinite beam are observed to be close. The maximum central deflection for case of 10 m beam is about 8% higher than that of the infinite beam. The effect of load positions on the central moment is depicted in Fig. 8. The moments for the 20 m beam and infinite beam are observed to be very close, whereas the moments for the case of 10 m finite beam differ considerably when the load lies in the first or last one-third span. In the central one-third span, the central moments for all three beams are nearly the same.

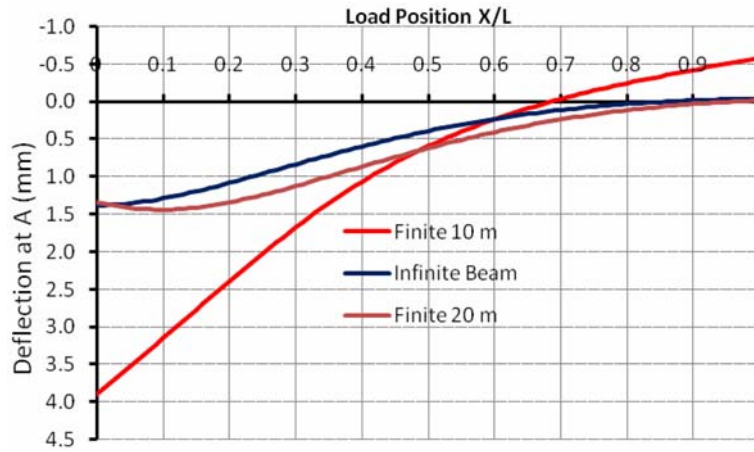


Fig. 6 Variation in end deflection against load position

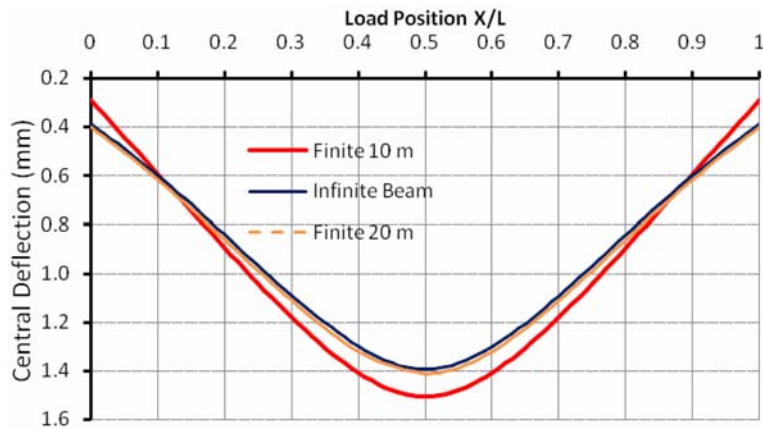


Fig. 7 Variation in central deflection against load position

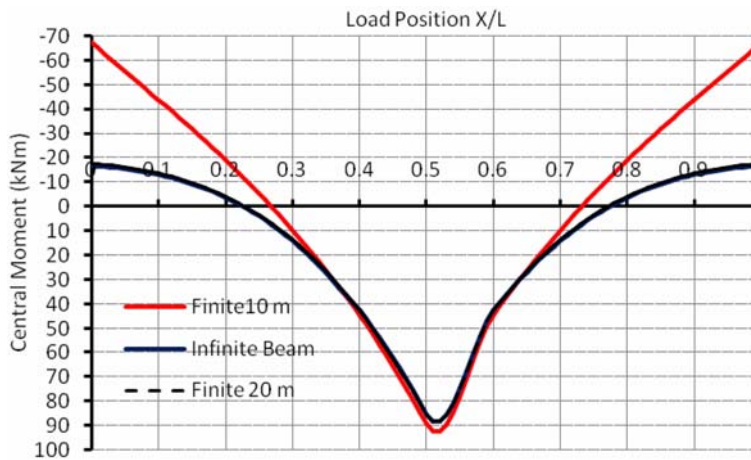


Fig. 8 Variation in central moment against load position

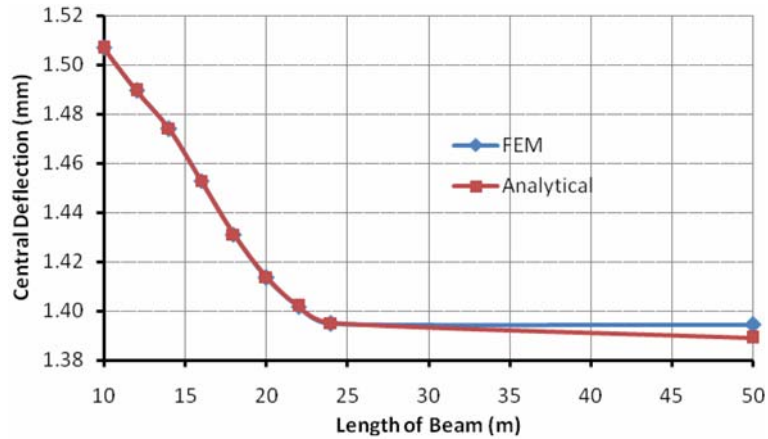


Fig. 9 Effect of length on central deflection

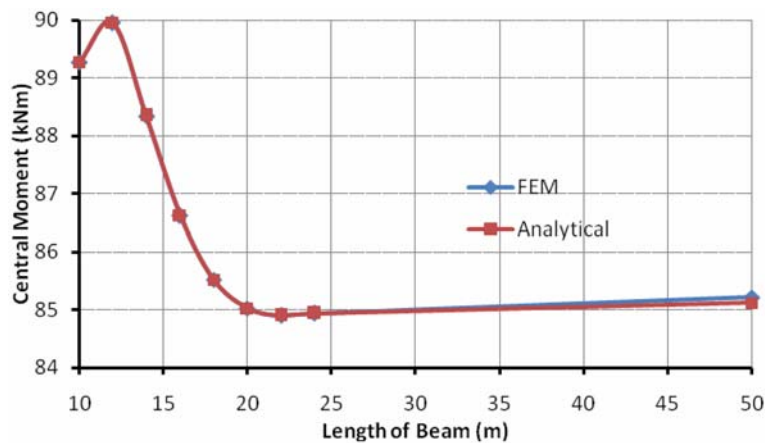


Fig. 10 Effect of length on central moment

5.2 Effect of beam length

The central deflection of the beam has been plotted against the length of the beam for the load applied at the central point in Fig. 9 along with the analytical result. As can be seen, good agreement exists between the two results. The central deflection approaches a constant when the beam length is over 24 m. Similar comparison for the central moment is presented in Fig. 10, which also indicates good agreement between the finite element analysis and analytical results. The moment increases up to 12 m and then decreases with further increase in beam length. Finally, it approaches a constant for the beam length over 20 m.

5.3 Effect of shear modulus G_p

While studying the effect of variations in shear modulus G_p , the soil modulus k was considered constant (10000 kN/m^3). The values of the shear modulus G_p adopted in the analysis are listed

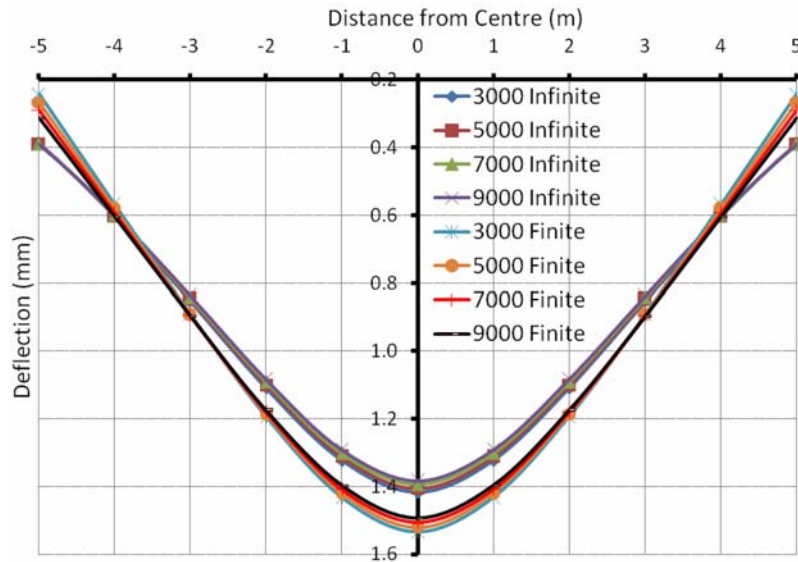


Fig. 11 Variation in deflection response under central load for different shear moduli G_p

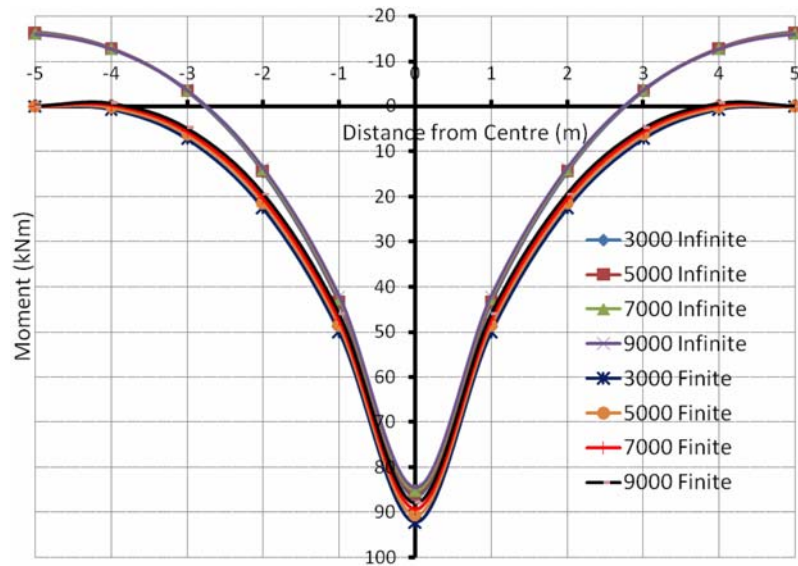
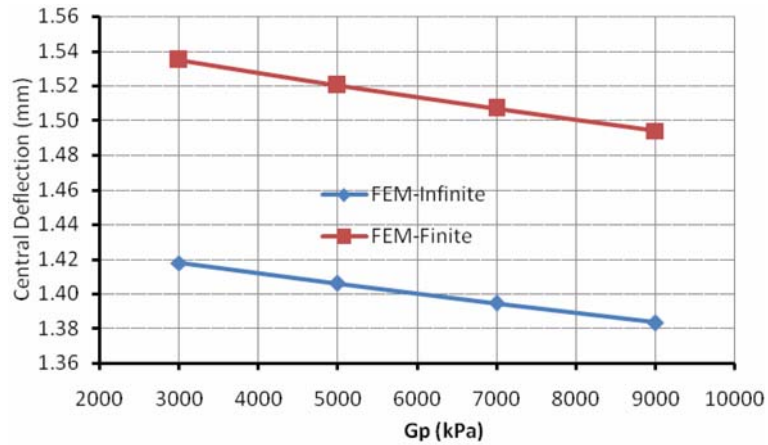
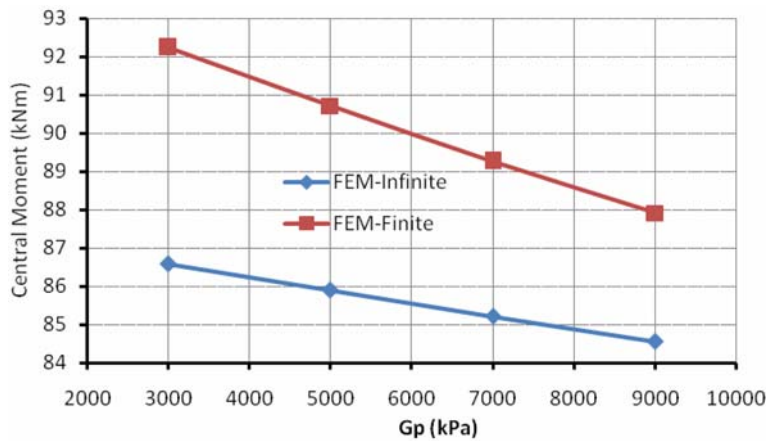


Fig. 12 Variation in moment response under central load for different shear moduli G_p

below: $G_p = 3000, 5000, 7000, 9000 \text{ kN/m}^2$. The deflection and bending moment curves under the central load are plotted for different values of G_p in Figs. 11 and 12, respectively. The effect of shear modulus G_p on the central deflection is plotted in Fig. 13. As can be seen, the central deflection decreases with the increase in shear modulus. Similar effect on the central moment is depicted in Fig. 14. The central moment decreases with the increase in shear modulus. Both the central deflection and moment are higher for finite beam as compared to the infinite beam.

Fig. 13 Effect of shear modulus G_p on central deflectionFig. 14 Effect of shear modulus G_p on central moment

6. Conclusions

This paper presents an improved solution algorithm based on the finite element method for the static analysis of rigid pavements under moving loads. The concrete pavement is discretized by finite and infinite beam elements. The infinite elements are suitable for modelling the far field with infinite domain. The underlying soil medium is modelled by the Pasternak model which takes into account the shear interaction between the spring elements. The deflections and moments of the beam under the central load are considered for validation. Very good agreement has been observed between the analytical and finite element results for the finite and infinite beams, which indicates the capability of modelling the infinite boundaries with the infinite elements developed here.

The parametric study conducted reveals that the central deflection and moment approach constant values with the increase in the beam length. With the increase in shear modulus, the central deflection and moment both decrease. Both the central deflection and moment are higher for finite beam as compared to the infinite beam.

References

- Bettess, P. (1977), "Infinite elements", *Int. J. Numer. Meth. Eng.*, **11**, 53-64.
- Foppl, A. (1992), *Vorlesungen uber technische Mechanik*, 258, Leipzig.
- Hetenyi, M. (1950), "A general solution for the bending of beams in an elastic foundation of arbitrary continuity", *J. Appl. Phys.*, **21**, 55.
- Hetenyi, M. (1946), *Beams on Elastic Foundation*, The University of Michigan Press, Ann Arbor, USA.
- Maheshwari, P., Chandra, S. and Basudhar, P.K. (1972), "Response of beams on a tensionless extensible geosynthetic-reinforced earth bed subjected to moving loads", *Comput. Geotech.*, **31**, 537-548.
- Mallik, A.K., Chandra, S. and Singh, A.B. (2006), "Steady-state response of an elastically supported infinite beam to a moving load", *J. Sound Vib.*, **291**, 1148-1169.
- Pasternak, P.L. (1954), *Fundamentals of a New Method of Analysis of an Elastic Foundation by Means of Two Foundation Constants* (in Russian), Gosudarstvennoe Izdatelstvo Literaturi po Stroitelstvu i Arkhitekture, Moscow.
- Selvadurai, A.P.S. (1979), *Elastic analysis of soil-foundation interaction Amsterdam*, Elsevier Scientific Publishing Company, The Netherlands.
- Shen, W. and Kirkner, D.J. (2001), "Nonlinear finite element analysis to predict permanent deformations in pavement structures under moving loads", *Int. J. Pavem. Eng.*, **2**, 187-199.
- Sun, L. (2001), "Dynamic displacement response of beam on elastic foundation for moving load", *Int. J. Solids Struct.*, **38**, 8869-8878.
- Sunitha, N.V., Dodagoudar, G.R. and Rao, B.N. (2008), "A fuzzy meshless method for beams on elastic foundation", *Indian Geotech. J.*, **38**(2), 119-139.
- Vlasov, V.Z. and Lbont'ev, N.N. (1966), *Beams, Plates, Shells on Elastic Foundation*, (translated from Russian), Israel Program for Scientific Translations, Available from the Clearinghouse of U.S. Dept. of Commerce.
- Winkler, E. (1867), *Die Lehre von der Elastizität und Festigkeit*, 182, Prague.
- Zimmermann, H. (1930), *Die Berechnung der Eisenbahnoberbaues*, 2nd Edition, Berlin.